

# 1 Coherent DVCS off $^4\text{He}$ : kinematics

In the following, we list the results appearing in *Coherent deeply virtual Compton scattering off  $^4\text{He}$* , Phys. Rev. C98 015203 (2018).

## 1.1 $x_B$ bins

$x_B$	$\langle Q^2 \rangle$ [GeV $^2$ ]	$\langle t \rangle$ [GeV $^2$ ]	$\text{Re}(\mathcal{H})$	$\text{Im}(\mathcal{H})$	$A_{LU} (90^\circ)$
0.132	1.18	-0.095	-9.92	31.64	0.253
0.171	1.45	-0.099	-6.89	22.50	0.267
0.225	1.84	-0.106	-6.95	15.27	0.272

Table 1:  $A_{LU}$  for average values of  $Q^2$  and  $t$  in  $x_B$  bins.

## 1.2 $Q^2$ bins

$Q^2$ [GeV $^2$ ]	$\langle x_B \rangle$	$\langle t \rangle$ [GeV $^2$ ]	$\text{Re}(\mathcal{H})$	$\text{Im}(\mathcal{H})$	$A_{LU} (90^\circ)$
1.15	0.134	-0.096	-10.66	31.60	0.279
1.42	0.171	-0.099	-7.40	22.73	0.278
1.87	0.223	-0.106	-7.28	15.53	0.275

Table 2:  $A_{LU}$  for average values of  $x_B$  and  $t$  in  $Q^2$  bins.

## 1.3 $t$ bins

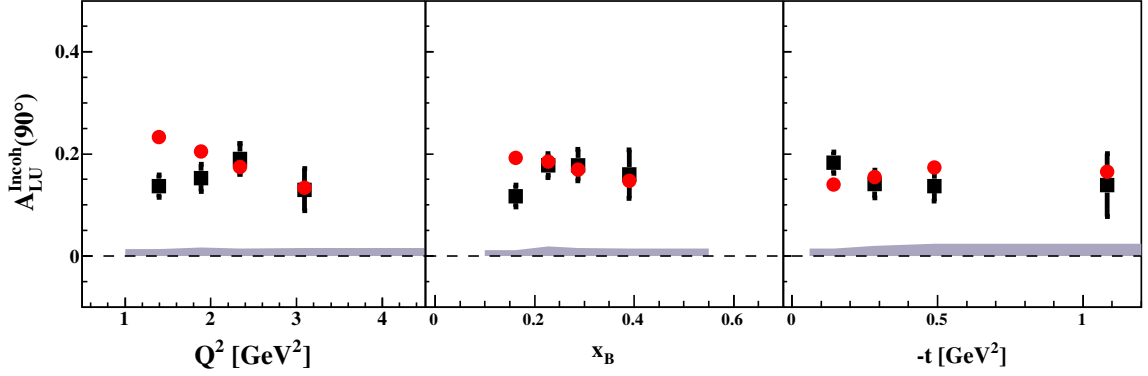
$t$ [GeV $^2$ ]	$\langle x_B \rangle$	$\langle Q^2 \rangle$ [GeV $^2$ ]	$\text{Re}(\mathcal{H})$	$\text{Im}(\mathcal{H})$	$A_{LU}(90^\circ)$
-0.081	0.159	1.37	-1.83	36.54	0.315
-0.094	0.179	1.51	-7.86	22.59	0.264
-0.126	0.193	1.61	-5.17	15.04	0.291

Table 3:  $A_{LU}$  for average values of  $x_B$  and  $Q^2$  in  $t$  bins.

## 2 Incoherent DVCS off $^4\text{He}$

### 2.1 $A_{LU}$

In the following, we list the results presented in our work *Catching a glimpse of the parton structure of the bound proton*, arXiv:1909.12261[nucl-th].



#### 2.1.1 $Q^2$ bins

$Q^2$ [GeV $^2$ ]	$\langle x_B \rangle$	$\langle t$ [GeV $^2$ ]	$\langle -\Delta^2/Q^2 \rangle$	$A_{LU}(90^\circ)$
1.40	0.166	-0.407	0.290	0.233
1.89	0.233	-0.499	0.264	0.205
2.34	0.290	-0.521	0.223	0.175
3.10	0.379	-0.650	0.210	0.134

Table 4:  $A_{LU}$  for average values of  $x_B$  and  $t$  in  $Q^2$  bins.

#### 2.1.2 $x_B$ bins

$x_B$	$\langle Q^2$ [GeV $^2$ ]	$\langle t$ [GeV $^2$ ]	$\langle -\Delta^2/Q^2 \rangle$	$A_{LU}(90^\circ)$
0.162	1.43	-0.397	0.278	0.192
0.227	1.93	-0.418	0.217	0.185
0.287	2.35	-0.492	0.209	0.169
0.390	2.99	-0.714	0.239	0.147

Table 5:  $A_{LU}$  for average values of  $Q^2$  and  $t$  in  $x_B$  bins.

### 2.1.3 $t$ bins

$t$ [GeV <sup>2</sup> ]	$\langle x_B \rangle$	$\langle Q^2$ [GeV] <sup>2</sup> $\rangle$	$\langle -\Delta^2/Q^2 \rangle$	$A_{LU}(90^\circ)$
-0.145	0.213	1.82	0.080	0.140
-0.282	0.255	2.13	0.132	0.155
-0.490	0.284	2.31	0.212	0.173
-1.11	0.308	2.41	0.461	0.165

Table 6:  $A_{LU}$  for average values of  $x_B$  and  $Q^2$  in  $t$  bins.

## 2.2 Ratios

In the following, we show the values of the ratio between the BSA of a moving proton and one at rest, respectively (from arXiv:1909.12261[nucl-th]).

$$R_{\mathcal{I}} = \frac{1}{\mathcal{N}} \frac{A \int d\vec{p} \int dE P^{^4He}(\vec{p}, E) g(\vec{p}, E, K) s_{Int}^{moving}(\vec{p}, E, K)}{J s_{Int}^{rest}(K)} \quad (1)$$

$$R_{BH} = \frac{1}{\mathcal{N}} \frac{A \int d\vec{p} \int dE P^{^4He}(\vec{p}, E) g(\vec{p}, E, K) \sum_i c_{i BH}^{moving}(\vec{p}, E, K)}{J \sum_i c_{i BH}^{rest}(K)} \quad (2)$$

$$R_{ALU} = \frac{R_{\mathcal{I}}}{R_{BH}} \quad (3)$$

where  $K, J, A$  are different combinations of the kinematical variables while  $\mathcal{N}$  accounts for the proper normalization in the considered bin.

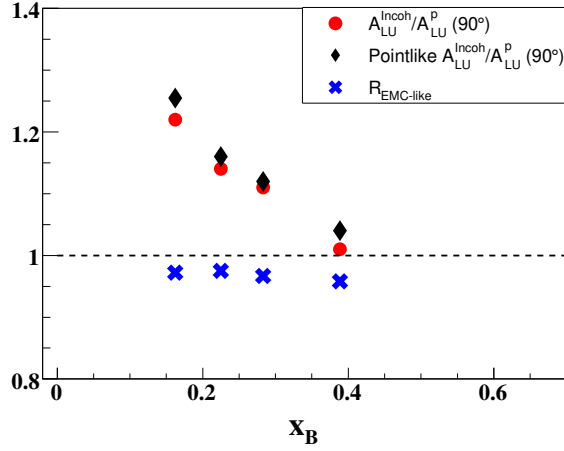


Figure 1: Ratio  $R_{ALU}$ .

### 2.2.1 $x_B$ bins

$x_B$	$R_{ALU}$
0.163	1.22
0.225	1.15
0.283	1.11
0.388	1.03

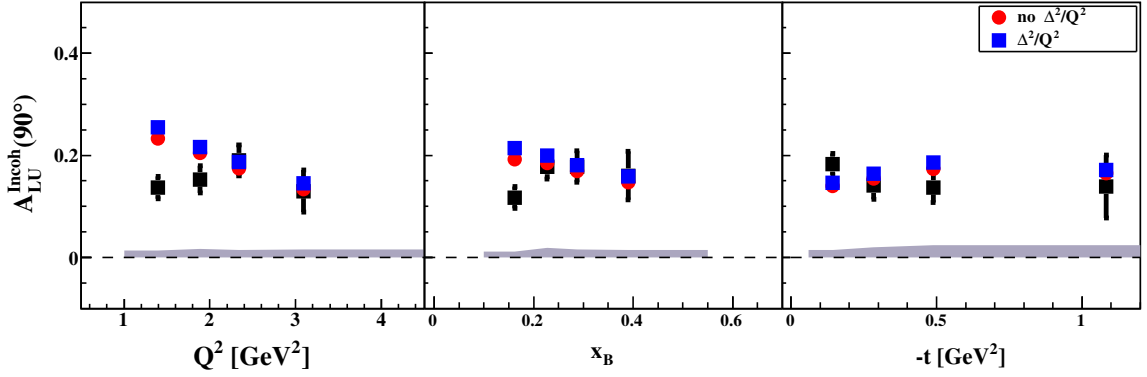
Table 7: Ratio given by Eq. (3) in  $x_B$  bins (red dots in Fig. 1).

### 2.3 Effects of terms of order $\Delta^2/Q^2$ in our asymmetries

We use now the complete expression for the skewness appearing in the CFF of the interference amplitude

$$\xi = \frac{Q^2(1 + \frac{\Delta^2}{2Q^2})}{2q \cdot P} \quad (4)$$

where  $q(P)$  is the average photon (proton) momenta and  $\Delta^2 = t$ . This accounts for the inclusion of all corrections of order  $t/Q^2$ , up to contributions from other GPDs which have still to be included (work in progress).



#### 2.3.1 $Q^2$ bins

$Q^2$ [GeV <sup>2</sup> ]	$\langle x_B \rangle$	$\langle t \rangle$ [GeV <sup>2</sup> ]	$\langle -\Delta^2/Q^2 \rangle$	$A_{LU}(90^\circ)$
1.40	0.166	-0.376	0.269	0.2477
1.89	0.233	-0.415	0.220	0.2241
2.34	0.288	-0.492	0.210	0.1918
3.10	0.379	-0.634	0.205	0.1463

Table 8:  $A_{LU}$  for average values of  $x_B$  and  $t$  in  $Q^2$  bins.

### 2.3.2 $x_B$ bins

$x_B$	$\langle Q^2 \text{ [GeV}^2] \rangle$	$\langle t \text{ [GeV}^2] \rangle$	$\langle -\Delta^2/Q^2 \rangle$	$A_{LU}(90^\circ)$
0.162	1.43	-0.397	0.278	0.2084
0.227	1.93	-0.418	0.217	0.203
0.287	2.35	-0.492	0.209	0.1847
0.390	2.99	-0.714	0.239	0.1625

Table 9:  $A_{LU}(90^\circ)$  for average values of  $Q^2$  and  $t$  in  $x_B$  bins.

### 2.3.3 $t$ bins

$t \text{ [GeV}^2]$	$\langle x_B \rangle$	$\langle Q^2 \text{ [GeV}^2] \rangle$	$\langle -\Delta^2/Q^2 \rangle$	$A_{LU}(90^\circ)$
-0.145	0.213	1.82	0.080	0.1455
-0.282	0.255	2.13	0.132	0.1644
-0.490	0.284	2.31	0.212	0.1902
-1.11	0.308	2.41	0.461	0.1728

Table 10:  $A_{LU}$  for average values of  $x_B$  and  $Q^2$  in  $t$  bins.

## 2.4 Ratios with terms of order $\Delta^2/Q^2$

$$R_{\mathcal{I}} = \frac{1}{\mathcal{N}} \frac{A \int d\vec{p} \int dE P^{4He}(\vec{p}, E) g(\vec{p}, E, K) s_{Int}^{moving}(\vec{p}, E, K)}{J s_{Int}^{rest}(K)} \quad (5)$$

$$R_{BH} = \frac{1}{\mathcal{N}} \frac{A \int d\vec{p} \int dE P^{4He}(\vec{p}, E) g(\vec{p}, E, K) \sum_i c_{iBH}^{moving}(\vec{p}, E, K)}{J \sum_i c_{iBH}^{rest}(K)} \quad (6)$$

$$R_{ALU} = \frac{R_{\mathcal{I}}}{R_{BH}} \quad (7)$$

where  $K, J, A$  are different combinations of the kinematical variables while  $\mathcal{N}$  accounts for the proper normalization in the considered bin. With respect to the ratio shown in section 2.2, effects appear in the definition (4) of the skewness variable and in the expression for the nucleon at rest.

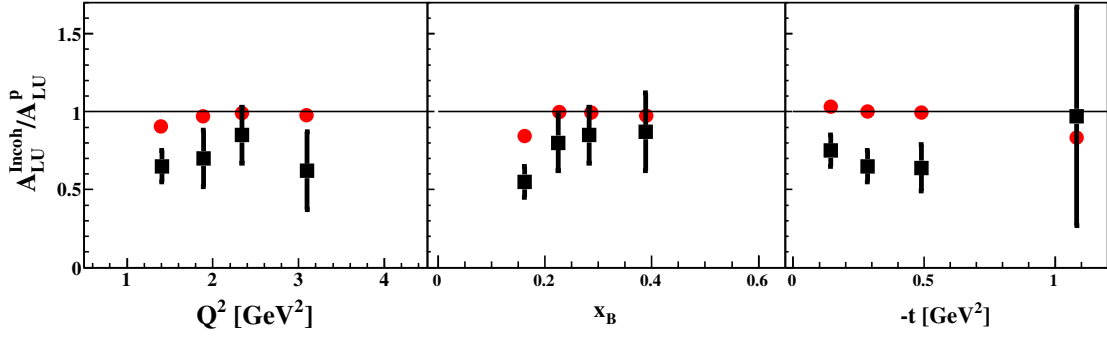


Figure 2: Comparison between our result for  $R_{ALU}$  and data from EG6 internal note.

### 2.4.1 $Q^2$ bins

$Q^2$ [GeV <sup>2</sup> ]	$R_{\mathcal{I}}$	$R_{BH}$	$R_{ALU}$
1.40	1.3616	1.5180	0.9038
1.89	1.2801	1.3216	0.9687
2.34	1.1434	1.1537	0.9904
3.09	1.0563	1.0823	0.9759

Table 11: Ratios given by Eqs. (5), (6), (7) in  $Q^2$  bins.

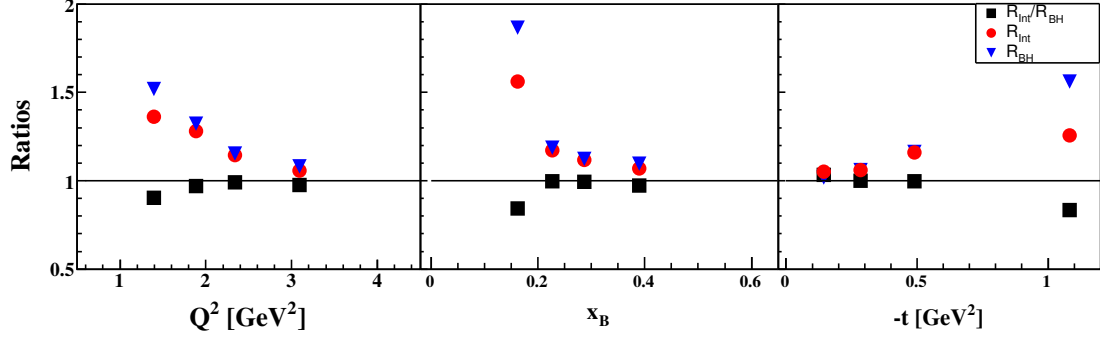


Figure 3: Our results for  $R_{\mathcal{I}}$ ,  $R_{BH}$  and  $R_{ALU}$ .

#### 2.4.2 $x_B$ bins

$x_B$	$R_{\mathcal{I}}$	$R_{BH}$	$R_{ALU}$
0.163	1.5604	1.8653	0.8430
0.225	1.1832	1.1860	0.9967
0.283	1.1172	1.1237	0.9937
0.388	1.0681	1.0963	0.9742

Table 12: Ratios given by Eqs. (5), (6), (7) in  $x_B$  bins.

#### 2.4.3 $-t$ bins

$t$ [GeV <sup>2</sup> ]	$R_{\mathcal{I}}$	$R_{BH}$	$R_{ALU}$
-0.136	1.0506	1.0178	1.0328
-0.281	1.0614	1.0606	1.0006
-0.492	1.1604	1.1641	0.9959
-1.090	1.2576	1.5605	0.8344

Table 13: Ratios given by Eqs. (5), (6), (7) in  $-t$  bins.



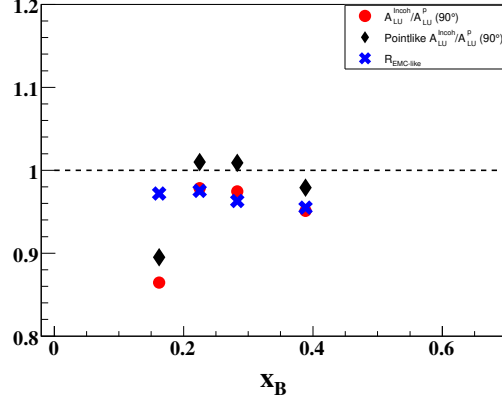


Figure 4: Zoomed  $R_{ALU}$ ,  $R_{EMC-like}$ ,  $R_{ALU}^{pointlike}$  in  $x_B$  bins.

### 3 $A_{LU}$ for a proton at rest: effects of $\mathcal{O}(\Delta^2/Q^2)$

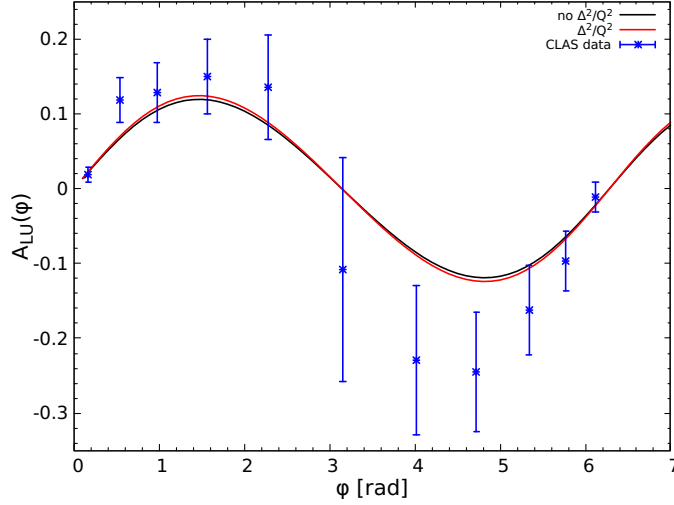


Figure 5: Beam spin asymmetry for a proton at rest considering (red curve) and ignoring (black curve) terms of order  $\Delta^2/Q^2$  in the interference part. In this kinematics ( $Q^2=1.31 \text{ GeV}^2$ ,  $\langle x_B \rangle=0.19$ ,  $\langle -t \rangle=0.15 \text{ GeV}^2$ ),  $\Delta^2/Q^2$  is 0.115.

Data (blue stars) from CLAS Coll., Stepanyan, PRL 87 (2001) 182002.

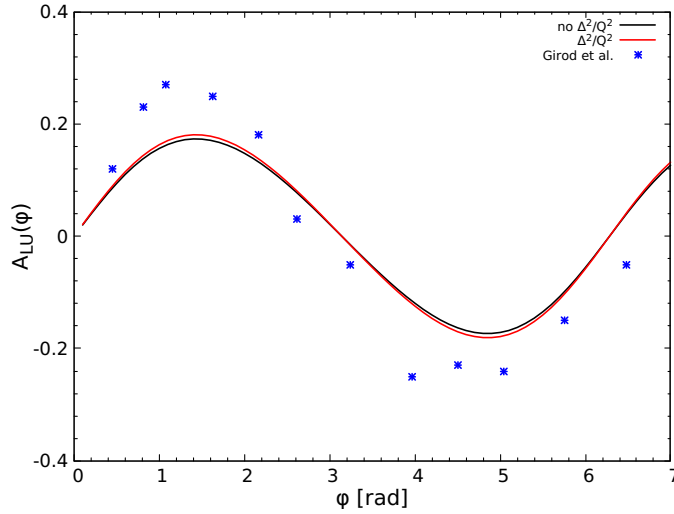


Figure 6: Beam spin asymmetry for a proton at rest considering (red curve) and ignoring (black curve) term of order  $\Delta^2/Q^2$  in the interference part. In this kinematics ( $Q^2=1.95 \text{ GeV}^2$ ,  $\langle x_B \rangle=0.25$ ,  $\langle -t \rangle=0.28 \text{ GeV}^2$ ),  $\Delta^2/Q^2$  is 0.144.

Data (blue stars) from CLAS Coll., Girod PRL 100 (2008) 162002.

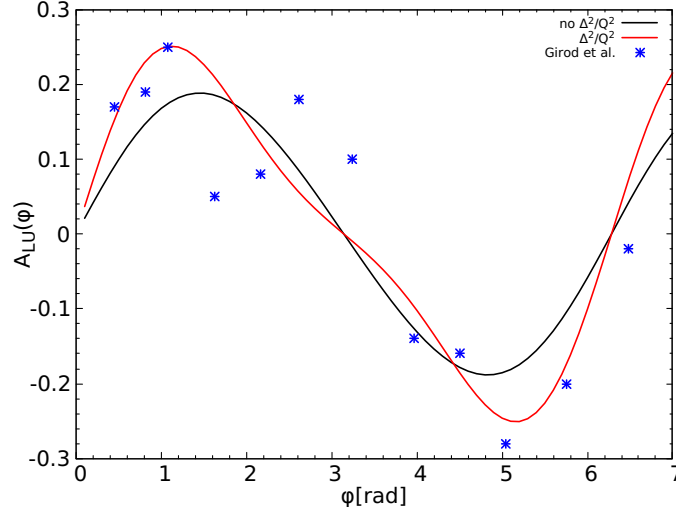


Figure 7: Beam spin asymmetry for a proton at rest considering (red curve) and ignoring (black curve) term of order  $\Delta^2/Q^2$  in the interference part. In this kinematics ( $Q^2=1.95$  GeV $^2$ ,  $\langle x_B \rangle=0.25$ ,  $\langle -t \rangle=0.49$  GeV $^2$ ),  $\Delta^2/Q^2$  is 0.25. Data (blue stars) from CLAS Coll., Girod PRL 100 (2008) 162002.

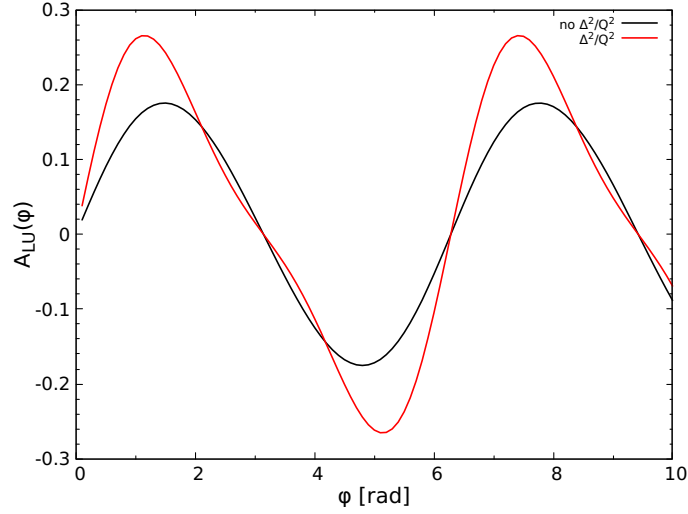


Figure 8: Beam spin asymmetry for a proton at rest considering (red curve) and ignoring (black curve) term of order  $\Delta^2/Q^2$  in the interference part. Kinematics ( $Q^2=1.45$  GeV $^2$ ,  $x_B=0.163$ ,  $\langle -t \rangle=0.374$  GeV $^2$ ) correspond to the former point in the  $x_B$  plot for  $A_{LU}$  from Hattawy, Phys. Rev. Lett. 123 (2019) 032502. For the considered point,  $\Delta^2/Q^2$  is 0.257.

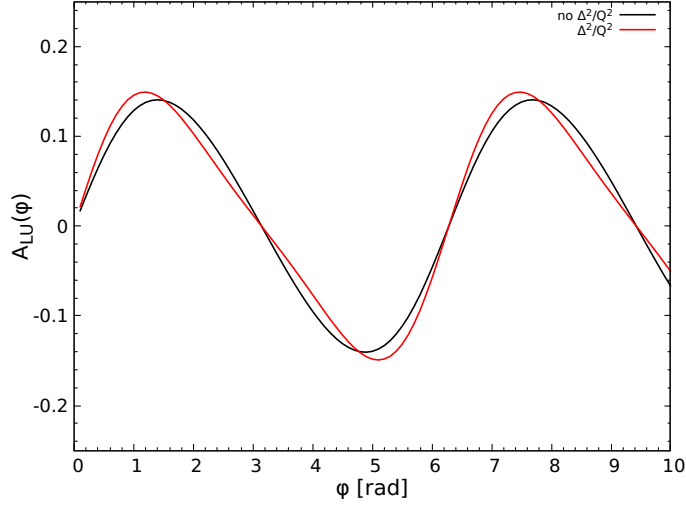


Figure 9: Beam spin asymmetry for a proton at rest considering (red curve) and ignoring (black curve) term of order  $\Delta^2/Q^2$  in the interference part. Kinematics ( $Q^2=1.84 \text{ GeV}^2$ ,  $\langle x_B \rangle=0.215$ ,  $-t=0.136 \text{ GeV}^2$ ) correspond to the former point in the  $-t$  plot for  $A_{LU}$  from Hattawy, Phys.Rev.Lett. 123 (2019) 032502. For the considered point,  $\Delta^2/Q^2$  is 0.074.

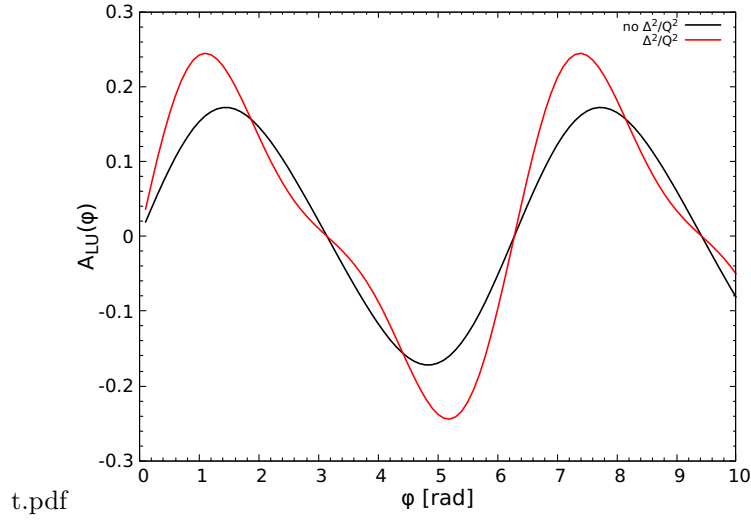


Figure 10: Beam spin asymmetry for a proton at rest considering (red curve) and ignoring (black curve) term of order  $\Delta^2/Q^2$  in the interference part. Kinematics ( $Q^2=2.44 \text{ GeV}^2$ ,  $\langle x_B \rangle=0.311$ ,  $-t=1.09 \text{ GeV}^2$ ) correspond to the last point in the  $-t$  plot for  $A_{LU}$  from Hattawy, Phys.Rev.Lett. 123 (2019) 032502. For the considered point,  $\Delta^2/Q^2$  is 0.447.